

NEW INSIGHTS FROM CSC/SDSS SPECTROSCOPIC GALAXIES

THE STAR-FORMATION/ACCRETION

SEQUENCE: Low-luminosity emission-line nuclei with AGN-like behavior might be the most common mechanism of cosmic black hole growth. Our understanding of the AGN population and their cosmic evolution thus rely heavily on investigations of these $z \approx 0$ systems, for example the ubiquitous narrow-lined Low Ionization Nuclear Emission Regions (LINERs, Ls) and the “transition” (T) objects that straddle the borders between starburst galaxies and AGN. Optical emission-line ratio diagnostics (the BPT diagram e.g., Baldwin81, Kewley06). for identifying the dominant ionization mechanism as either accretion or star-formation remain inconclusive for the majority of Ls and Ts . Analysis of the optical emission properties of these low luminosity AGN (LLAGN) in relation to a wide variety of characteristics of their hosts and large scale environments [Constantin06, Constantin08, Schawinski07] suggest an evolutionary sequence $H\text{II} \rightarrow S/T \rightarrow L$. The hydrodynamical models show that supermassive black hole (SMBH) accretion peaks considerably *after* the merger starts, and *after* the SFR has peaked [e.g., diMatteo05, Hopkins06]. Mergers that eventually breed massive “red and dead” passive ellipticals may occasionally still harbor active nuclei (the so-called X-ray bright, optically normal galaxies, or XBONGs, e.g., Civano07). Constraining the nature of this sequence at $z \sim 0$ will improve our understanding of whether/how the local LLAGN phenomenon fits into the SMBH/spheroid co-evolution paradigm. However, X-rays provide a crucial complement, since X-ray emission is a far more reliable signature of accretion activity than are optical emission lines. For normal galaxies, X-rays also provide a key measure of star formation history by tracing the accreting X-ray binary (XRB) populations.

Our understanding of the inter-relationship of star formation and accretion in the nearby universe can be greatly enhanced only with a truly large sample of objects with both detailed op-

tical spectroscopic and X-ray information available. We describe below the best available SDSS/Chandra galaxy sample and our unique analysis of it. We outline several key science projects we will undertake, but many more will be facilitated by our commitment to publishing fit results for the full sample.

DEFINING OUR GALAXY SAMPLE:

We have cross-correlated and visually validated over 800 positional matches between the Chandra Source Catalog (CSC; Evans09) and the SDSS DR7 spectroscopic catalog, for SDSS galaxies and AGN with $z < 0.38$ (allowing $H\alpha$ region diagnostics). Images and spectra of our sample - the 615 unambiguous matches with high quality X-ray data (e.g., pileup $< 10\%$) - can be seen at <http://www.cscsdss.appspot.com/sdss>. Of these galaxies, 85% occur serendipitously in the Chandra field.

STRENGTH IN DIVERSITY. Our full galaxy sample spans a wide range of host masses, stellar populations, black hole masses, AGN luminosities and obscuration. For normal galaxies, the X-ray emission arises from accreting binaries (HMXBs in young stellar populations, LMXBs from older populations) or from hot ISM (mostly in elliptical galaxies). AGN (QSOs, Sy1, Sy1.x, Sy2) show primarily power-law X-ray emission from the accretion disk/corona surrounding the SMBH. Low-luminosity AGN (LLAGN), including the Low-Ionization Nuclear Emission-line Region (LINER) and Transition galaxies often show a mix of the above components. Our detailed optical spectroscopic modelling, described below, begins to tell us the mix of AGN and stellar population components in the optical. However, low-luminosity accretion power may go undetected in the optical, especially where obscuration or radiatively inefficient accretion (RIAF) applies, making L_X and the X-ray spectral shapes crucial to probe beneath the veil. We expect this study to sprout many productive branches, of which we sketch just three below.

A KEY TEST FOR SMBH/X-RAY BINARY ANALOGIES. We recently unveiled a strong double-sloped correlation of Γ vs. L/L_{Edd} among AGN (Figure 1; Constantin09).

The AGN sample trend is crisply mirrored by *individual* accreting X-ray binaries (XRBs and ULXs; Wu08). Such striking physical connections over 5 – 8 orders of magnitude in BH mass demand further investigation, a primary goal of this proposal. Our ChaMP sample of 107 galaxies (Constantin09) produced groundbreaking results, but with caveats. First, the softer (larger Γ), mostly passive galaxies, could simply be poor power-law fits to soft thermal plasma component, Second, we were forced to mix results from published optical spectroscopic fits from MPA/JHU for galaxies (Tremonti04) with Shen et al. (2008) for Sy1 and QSOs. The Narrow Line Sy1 were excluded entirely. The current CSC/SDSS study will now expand the sample to 630 objects, with (median) $\sim 2.5\times$ more X-ray counts, and with fully consistent optical spectroscopic fits across *all* galaxy/AGN types.

NARROW LINE SEYFERT 1s.

NLS1 tend to have narrow $H\beta$ broad line components ($\lesssim 2000 \text{ km s}^{-1}$), weak [OIII] lines, strong optical FeII emission, and be radio quiet. The strongest arguments to date link such properties to Eddington ratio L/L_{Edd} (Brandt98) and/or the orientation of a disc-like broad line region (BLR; Sulentic00, Marziani01). Most commonly, NLS1 are posited to be “young” SMBH with small black hole masses and high L/L_{Edd} (Borson02, Grupe04), but other models invoking e.g., orientation (DeCarli08) and/or warm (ionized) outflowing absorbers (Done07, Sobolewska07) offer strong challenges. Key to resolving these debates is an unbiased NLS1 sample. Why? NLS1 are generally thought to be X-ray soft and loud (steep X-ray power-law slope Γ and flat α_{ox} ,¹ respectively). However, the majority of past, rather intensively studied NLS1 samples were selected in the shallow soft (0.5 - 2 keV) ROSAT All Sky Survey (RASS). We hypothesize that many were *flaring*, which is consistent with these facts: (a) strong variability is expected for high L/L_{Edd} (Wilhite08, McHardy10), (b) Sy1 get softer as they flare (Sobolewska09) and (c) 17 RASS-undetected NLS1 observed with Chan-

dra showed a much wider range of Γ and L_X (Grupe04). This flaring hypothesis is now fully confirmed by recent *Swift* observations of NLS1 (Grupe10), wherein the majority of NLS1 are fainter than in the RASS.

Since the reported SEDs and the variability of NLS1 have all been strongly affected by this bias, we propose to study the multiwavelength properties of an optically-selected sample of NLS1 with much-reduced bias, and more representative overall SEDs. From our CSC/SDSS sample, about 45 objects emerge as NLS1 when we require significant broad components in $H\beta$ and $H\alpha$, both with $\text{FWHM} < 2000 \text{ km/s}$.² Only 2 of these were Chandra PI targets.

If NLS1 are indeed in a high accretion phase, they should fall at the steep Γ , high L/L_{Edd} end of the trend in Figure 1, analogous to the soft/high state of XRBs. Extant RASS-dominated soft NLS1 samples are strongly biased against absorbing outflows. If NLS1 are high L/L_{Edd} , our CSC/SDSS sample may be expected to reveal signs of outflows. We will test for emission line centroids or skews blueshifted from the systemic redshift (Komossa08), which in turn should correlate with X-ray absorption signatures.

MORPHOLOGY and MERGERS. It is now obvious that galaxies regularly merge and that SMBH reside in the centers of effectively all galaxies with bulges (e.g., Richstone98). These two facts alone suggest that merging galaxies with active AGN should be extremely common (e.g., Begelman et al. 1980). For our CSC/SDSS sample, we use a morphological classification system similar to GalaxyZoo2 (Schawinski10), using the identical image scale and stretch, and we classify objects into elliptical, lenticular, spiral, (with subcategories of inclination), irregular, disturbed, multiple, etc. We find 31 significantly disturbed systems. Such mergers are expected to yield enhanced star-formation and accretion activity. Accounting for those (13) well-known interacting systems that were Chandra PI tar-

¹The hypothetical UV-to-X-ray power-law index $\alpha_{\text{ox}} = 0.384 \log(L_{2500\text{\AA}}/L_{2\text{keV}})$. ‘Flat’ means X-ray bright.

²Additional restrictions (e.g., [OIII]/ $H\beta < 3$) to distinguish from Sy 2s used in some previous studies are no longer required at our resolution and S/N.

gets such as Mrk 463, Mrk 266, and The Mice.³ mergers do *not* appear to be over-represented in our X-ray sample, relative to the overall Galaxy-Zoo fraction (Darg10). However, several of the newly-studied systems have multiple optical nuclei and hints of corresponding multiple X-ray nuclei, indicative of AGN triggering. Some hints of morphology-related trends may appear in Figure 2 such as excess absorption in mergers, an absorption trend with inclination in spirals, etc. However, these must be teased out carefully from processes related to AGN- and star-formation, as is only conceivable with a large sample: 414 of our galaxies are resolved and have preliminary classifications.

MULTIWAVELENGTH ANALYSIS:

SDSS Spectra. We decompose the SDSS spectra as described in Zhou et al. (2006), beginning with starlight (using galaxy templates of Lu06) and nuclear emission (power-law) components that also include reddening, Fe II template and Balmer continuum fitting. Iterative emission line fitting follows, using multiple Gaussian or Lorentzian profiles where warranted to fit broad and narrow line components. Emission line ratios (BPT diagram) provides optical diagnostics for AGN vs. starburst activity. We estimate stellar mass from the velocity dispersions σ_* of the broadened galaxy templates, and use the $H\delta_A$ Balmer absorption-line index as a proxy for the age of the associated stellar population (Kauffmann03). Black hole mass is estimated for BLAGN from FWHM($H\beta$) (Vestergaard06).

Chandra Analysis. We fit all X-ray spectra with redshift and N_H^{Gal} frozen for two minimal models - a simple power-law yielding best-fit photon index Γ , or an intrinsic absorbing column N_H^{intr} , by freezing Γ to the ~ 1.8 typical of AGN or XRBs. We thus measure at minimum one X-ray spectral parameter and f_X , L_X and f_X/f_{opt} . With the median number of counts (50), a simultaneous fit to Γ with ± 0.3 and intrinsic N_H to an upper limit of $\sim 10^{21} \text{ cm}^{-2}$ (both at 90% confidence). For ($\gtrsim 200$) we can begin to investigate partial covering for N_H^{intr} as well. An underlying

power-law is suitable for fitting both SMBH accretion and X-ray binary populations.⁴ For diffuse thermal gas (hot ISM) emission, we fit an APEC⁵ thermal model, starting with temperature frozen at 0.7 keV (e.g., Ptak99). For the (78) objects observed in multiple Chandra obsids, all data are included in the fits.

The unprecedented size and quality of our sample is what will allow us to explore several novel but important further analyses.

* (1) *Best Optical-Blind X-ray Fit.* We will attempt to choose for each galaxy the X-ray spectral model *justified by the X-ray data alone*, using an equivalent of $\Delta\chi^2$ for model comparisons that does not require binning the X-ray photons, is valid into the low-counts regime, and fully accounts for the number of parameters in each model. X-ray model comparisons will be implemented in CIAO/Sherpa 4.2 with the Cash maximum likelihood function (Cash79), and the `cstat` statistic, but we will need to obtain goodness-of-fit measures by performing Monte Carlo simulations, to repeatedly sample new datasets from the best-fit model to derive where the observed Cash statistic lies within the derived distribution of Cash statistics.

* (2) *Simultaneous Fits by Optical Class.* For galaxies with similar optical properties (e.g., by host mass, SFR, and/or) we will perform simultaneous X-ray spectra fitting. This method rigorously accounts for the individual redshifts and N_H^{Gal} , along with the separate PSF and (time-dependent) QEs for each Chandra observation. For instance, there are ~ 80 Sy2s in the sample, totalling 21,537 X-ray photons (over 2.9 Msec of exposure), which could themselves be divided into several bins of e.g., host mass and luminosity, and still allow for complex multicomponent X-ray spectral fits.

* (3) *Principal Component Analysis.* We also plan to use the optically-blind X-ray and the X-ray-blind optical spectroscopic modelling separately to create a multi-parameter eigenspace

³Very large, low-redshift spatially extended systems are not included in CSCv1.1

⁴Practically speaking, there is little hope of distinguishing a ~ 7 keV thermal bremsstrahlung from a $e\Gamma \sim 1.7$ power-law for the XRB emission.

⁵APEC is the Astrophysical Plasma Emission Code, see <http://cxc.harvard.edu/atomdb>.

that includes e.g., host galaxy mass from σ_V , starformation rate, BPT classification, nuclear power-law luminosity and reddening from the SDSS spectroscopic fits, and L_X and best X-ray spectral fit parameters (e.g., Γ , absorption, and the relative normalizations of power-law and APEC components) from Chandra. Principal Component Analysis should then reveal the eigenvectors (the orthonormal axes in the eigenspace that sequentially account for the largest remaining variance). The advantage of this method is that it can reveal unexpected relationships, and does not overweight the brighter flux sources.

* (4) *Optical Priors*. Galaxies are classified by optical spectroscopy first as BLAGN, emission line, or absorption line (“passive”) galaxies. The optical line ratio diagram further classifies emission line galaxies into starburst, LINER, Transition or Sy2 galaxies. The fitting constrains the observed (dereddened) ratio of starlight to optical AGN power-law continuum. Star-formation rates are available from our fits, and the X-ray/SFR correlations in the literature can be used to predict the thermal X-ray component.

SUMMARY OF PLANS:

* Measure best-fit X-ray spectral parameters of sample, for a variety of models. Develop MonteCarlo simulations to distinguish most appropriate optical-blind X-ray models.

* Measure optical spectra: overall stellar mass and age, AGN continuum, reddening of stellar and nuclear continuum components, emission and absorption line indices. Estimate M_{BH} and L_{Edd} .

* Perform simultaneous X-ray fits by optical class, test principal component analysis, and use of optical priors.

* Contrast optical reddening measures to N_H^{intr} from X-ray spectra to constrain dust/gas absorption (e.g., Blustin05). Test for trends with morphology.

* From optical emission line strengths and moments (centroid, width and asymmetry), correlate blueshifts and asymmetry with L/L_{Edd} . Does high L/L_{Edd} produce outflows?

* Measure α_{ox} , Γ , N_H^{intr} and X-ray variability for NLS1. Are NLS1 relatively X-ray bright, soft,

or flaring?

The PI will provide overall scientific direction and coordination. A. Constantin will investigate in particular the Γ vs. L/L_{Edd} correlation, and D.-W. Kim will oversee interpretation of the X-ray properties of normal galaxies. Aldcroft will lead X-ray spectral analysis of the full sample using `pyaxx` spectral fitting tool⁶, and he will also perform simultaneous spectral fitting for selected subsamples. Zhou will perform the detailed optical spectroscopic fits. The X-ray and optical images, spectra, and spectral fit results, as well as derived quantities like M_{BH} , L/L_{Edd} , will be released by November 2011 to the public.

BUDGET: The team is led by salaried scientists at the Chandra X-ray Center (CXC). For the projects discussed, we need 8 months continued support for a postdoc (\$40k). We also request funds for conference travel (1 domestic, 1 international) — \$5k and 20 ApJ pages (w/ 3 color figs) — \$2.8k. Our total request with health insurance and overhead is thus \$54k.

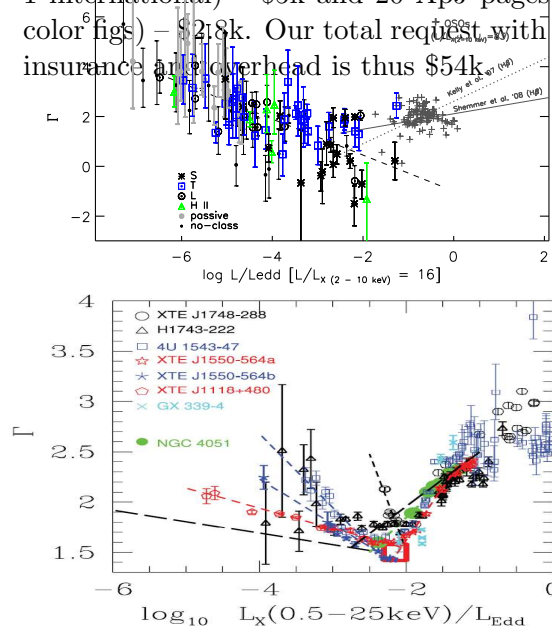
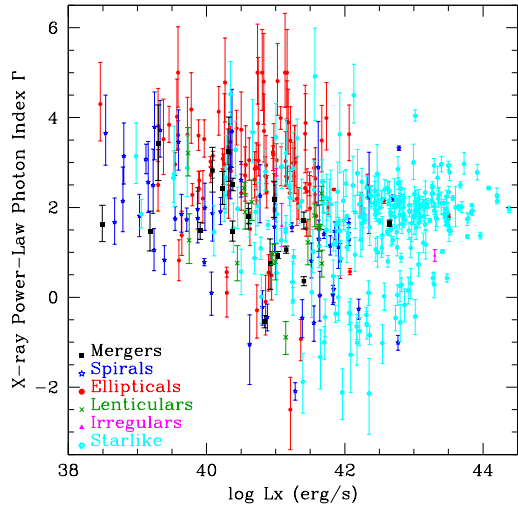


Figure 1: Correlations between the hard X-ray photon index Γ and the Eddington ratio. TOP: Our sample of 107 Chandra/SDSS galaxies and AGN (Constantin09) reveals a strong correlation, with a turnover near $\log L/L_{Edd} = -2$ between low luminosity AGN and QSOs. BOTTOM: Individual Galactic X-ray Binaries show strikingly similar trends when they vary (Wu08), suggesting similar accretion physics spanning 5 - 8 orders of magnitude in black hole mass.

⁶`pyaxx` is a similar tool we built for ChaMP which batch-processes X-ray spectra and is public at <http://cxc.harvard.edu/contrib/pyaxx>



2008, MNRAS, 383, 1232 **Wu**, Q. & Gu, M. 2008, ApJ, 682, 212 **Zhou**, H. et al. 2006, ApJS, 166, 128

Figure 2: The simplest X-ray spectral fit result, photon index Γ , is plotted against (0.5 - 7 keV) X-ray luminosity, with point types and colors distinguishing our preliminary *optical morphological* class for those 443 galaxies with the highest confidence classification. Without more detailed fits, Γ here merely represents “hardness”, which may either be intrinsic, or caused by absorption.

REFERENCES: **Baldwin**, J. A. Phillips, M. M., & Terlevich, R., 1981, PASP, 93, 5 **Begelman**, M. C., Blandford, R. D., & Rees, M. J. 1980, Nature, 287, 307 **Blustin**, A. J., et al. 2005, A&Ap, 431, 111 **Boroson**, T. A. 2002, ApJ, 565, 78 **Brandt**, N., & Boller, T. 1998, Astr. Nachr., 319, 7 **Cash**, W. 1979, ApJ 228, 939 **Civano**, F., et al. 2007, A&A, 476, 1223 **Constantin**, A., & Vogeley, M.S., 2006, ApJ, 650, 727 **Constantin**, A., et al. 2008, ApJ, 673, 715 **Constantin**, A., et al. 2009, ApJ, 705, 1336 **Darg**, D. W., et al. 2010, MNRAS, 401, 1043 **DeCarli**, R. et al. 2008, MNRAS, 386, L15 **di Matteo** et al 2005, Nature, 433, 604 **Done**, C. et al. 2007, MNRAS, 374, L15 **Evans**, I. et al. 2009, Proc., Chandra’s First Decade of Discovery, Eds Wolk, S., Fruscione, A., and Swartz, D., abstr #94 **Grupe**, D. 2004, AJ, 127, 1799 **Grupe**, D., et al. 2010, arXiv:1001.3140 **Hopkins**, P.F. & Hernquist, L., 2006, ApJ, 166, 1 **Kauffmann**, G., et al. 2003, MNRAS, 346, 105 **Kewley**, L.J., Groves, B., Kauffmann, G., & Heckman, T., 2006, MNRAS, 372, 961 **Komossa**, S., et al. 2008, ApJ, 680, 926 **Marziani**, P., 2001, ApJ, 558, 553 **McHardy**, I. 2010, LNIP, 794, 203 **Ptak**, A., et al. 1999, ApJS, 120, 179 **Richstone**, D., et al. 1998, Nature, 395, A14 **Schawinski**, K., et al. 2007, ApJs, 173, 512 **Schawinski**, K., et al. 2010, ApJ, 711, 284 **Shen**, Y., et al. 2008, ApJ, 680, 169 **Sobolewska**, M.A., et al. 2007, MNRAS, 374, 150 **Sobolewska**, M. & Papakis 2009, MNRAS, 399, 1597 **Sulentic**, J.W., et al. 2000, ApJL, 536, L5 **Tremonti**, C. A., et al. 2004, ApJ, 613, 898 **Vestergaard**, M., & Peterson, B. M. 2006, ApJ, 641, 689 **Wilhite**, B.C.,